Journal of Hydrology 490 (2013) 74–87

Contents lists available at SciVerse ScienceDirect

Journal of Hydrology

journal homepage: www.elsevier.com/locate/jhydrol

Natural saltwater upconing by preferential groundwater discharge through boils

P.G.B. de Louw [a,*], A. Vandenbohede [b], A.D. Werner [c], G.H.P. Oude Essink [a]

[a] Deltares, Dept. of Soil and Groundwater, P.O. Box 85467, 3508 AL Utrecht, The Netherlands
[b] Geology and Soil Science, Ghent University, Krijgslaan 281 (S8), 9000 Gent, Belgium
[c] National Centre for Groundwater Research and Training, School of the Environment, Flinders University, GPO Box 2100, Adelaide, SA 5001, Australia

ARTICLE INFO

Article history:
Received 15 November 2012
Received in revised form 27 February 2013
Accepted 21 March 2013
Available online 30 March 2013
This manuscript was handled by Corrado Corradini, Editor-in-Chief, with the assistance of Barbara Mahler, Associate Editor

Keywords:
Saltwater upconing
Boils
Preferential flow
Salinization
Seepage
Deep polder

SUMMARY

Natural saltwater upconing caused by the preferential groundwater discharge of boils is a key process in the salinization of Dutch deep polders. The factors controlling upconing by boil discharge and boil water salinities are poorly constrained and have not been previously documented. We addressed this knowledge gap by investigating upconing mechanisms using field measurements and numerical simulations of simplified situations. Boils occur as conduits in the upper aquitard connecting the underlying aquifer to the surface and allowing groundwater to discharge at rates up to 100 $m^3 d^{-1}$ with Cl concentrations up to 5 $g L^{-1}$. Boils are found as isolated features or clustered in small areas of 20–100 m^2. Field observations show that preferential flow through boils creates localized and narrow saltwater upconing spikes, causing the elevated boil water salinities. Modeling results indicate that boil water in Dutch polders comprises mixtures of groundwater from a wide range of depths and salinities with larger contributions from shallower and less saline groundwater than from the deeper and more saline water. Similar to previous numerical studies of pumping-induced upconing, the numerical results show that the most important factors controlling the boil salinity in Dutch polders are boil discharge, the horizontal hydraulic conductivity of the aquifer, the depth of the transition zone and the salinity (or density) contrast within the aquifer. When boils are clustered, natural saltwater upconing is a function of the total discharge of a boil cluster, whereas the boil-to-boil salinity variations within a cluster are determined by the discharge of individual boils and their position relative to neighboring boils. Regional lateral flow significantly modifies flow patterns by dividing the groundwater flow system into a local boil system overlying the regional flow system. Despite this, regional flow has only a minor effect on the relative contributions of saline and fresh groundwater to boil discharge and thus on boil salinity as well.

1. Introduction

In many deltaic areas, groundwater is saline because of the combined effects of seawater intrusion and marine transgressions (e.g. Custodio and Bruggeman, 1987; Post and Abarca, 2010). Saline groundwater in The Netherlands originates from Holocene transgressions producing a wide range of salinity distributions (Oude Essink, 1996; Post, 2004; Vos and Zeiler, 2008). Saline groundwater may reach the surface by upward groundwater flow (referred to here as seepage) in areas that lie below mean sea level (MSL). As one-quarter of The Netherlands lies below MSL, saline seepage leads to salinization of surface waters for large areas, impacting on agriculture and aquatic ecosystems (e.g. Van Rees Vellinga et al., 1981; Van der Eertwegh et al., 2006; Oude Essink et al., 2010). The largest seepage fluxes in The Netherlands are found in deep polders, which are reclaimed lakes. Surface waters in these systems are maintained at levels as low as 4–7 m below MSL, causing large upward and lateral hydraulic gradients in the underlying aquifers (e.g. Van Rees Vellinga et al., 1981; Oude Essink et al., 2010).

De Louw et al. (2010) showed that preferential seepage through boils is the dominant salinization source in deep polders in The Netherlands. In these systems, boils occur as conduits in the upper aquitard of peat and clay that connect the underlying aquifer to the surface, allowing groundwater to discharge at high velocities (Fig. 1). When the pressure of water in the aquifer is greater than the pressure exerted by the weight of the overlying stratum, heaving and cracking can occur, creating flow pathways that lead to the development of boils (Holzer and Clark, 1993; Li et al., 1996; TAC-FD (Technical Advisory Committee on Flood Defenses), 1999). About 85% of the boils mapped by De Louw et al. (2010) occurred in ditches and only 15% were found on dry land. Boils occurred either as single boils or as clusters of multiple boils within small

* Corresponding author. Tel.: +31 (0)6 30548000; fax: +31 (0)88 335 7856.
E-mail address: Perry.deLouw@deltares.nl (P.G.B. de Louw).

0022-1694/$ - see front matter © 2013 Elsevier B.V. All rights reserved.
http://dx.doi.org/10.1016/j.jhydrol.2013.03.025

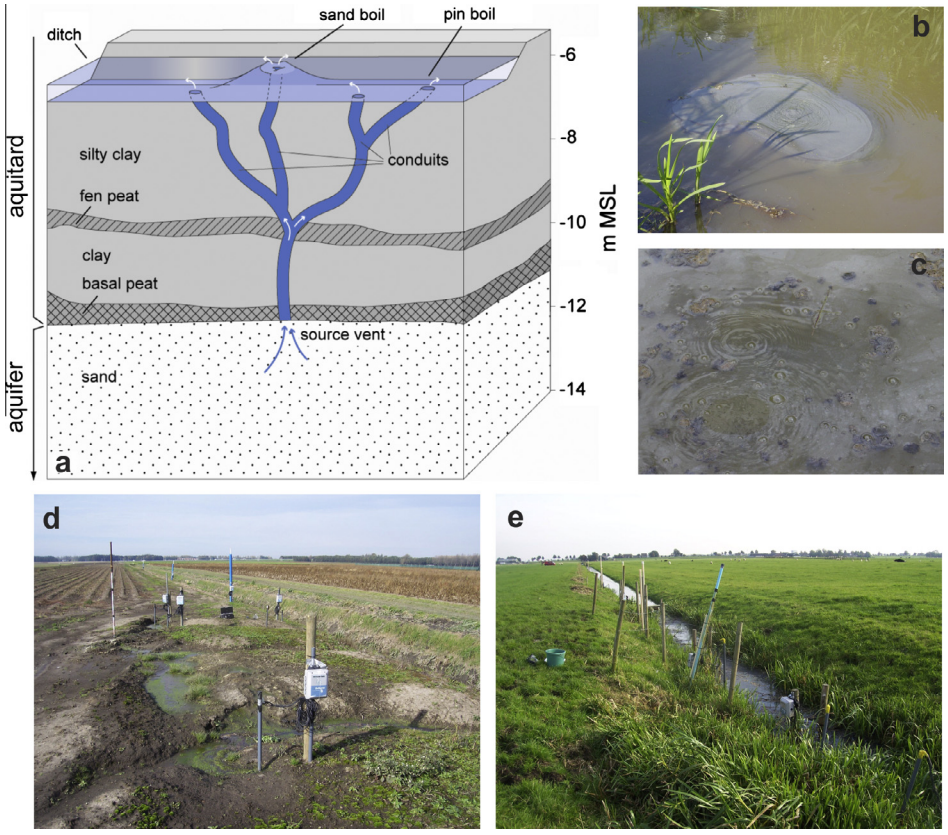

Fig. 1. Boils in deep polders: (a) diagram of boils with several conduits in aquitard (adapted from De Louw et al. (2010)), (b) sand boil, (c) a boil emitting methane, (d) study site A: boils on land and monitoring network, and (e) study site B: boils in ditch and monitoring network.

boil areas (<100 m^2). Individual boil fluxes ranged from 0.5 to 100 $m^3\ d^{-1}$. Field measurements by De Louw et al. (2010) showed that the salinities of boil discharge are much higher than that of diffuse seepage. Diffuse seepage is seen over the majority of the polder, whereby groundwater flows slowly upwards through the soil matrix of the upper aquitard's low-permeability sediments. For example, the median chloride (Cl) concentration of 49 boils in the deep Noordplas Polder was 1.3 $g\ L^{-1}$, whereas the median Cl concentration of diffuse seepage was 0.095 $g\ L^{-1}$ (De Louw et al., 2010). Larger boils with higher discharge rates tended to have higher Cl concentrations, i.e. up to 2.9 $g\ L^{-1}$. Over 200 boils were observed in the Haarlemmermeer Polder with variable salinities up to 5 $g\ L^{-1}$ of Cl (Goudriaan et al., 2011).

Based on field measurements, De Louw et al. (2010) concluded that natural upconing of deep, saline groundwater induced by local, high-velocity flows through boils is the mechanism that leads to high boil salinities. As a result, boils impart high salt loads to deep polder systems. This was demonstrated by De Louw et al. (2011a) for the Noordplas Polder, where boils contribute about 66% of the total salt load from only 15% of the total water flux. Despite that the importance of boils in the surface water salinization of deep polders has been clearly demonstrated, the associated saltwater upconing mechanisms remained largely unevaluated. Therefore, saltwater upconing mechanisms controlling boil salinities is the main focus of the present study.

Natural saltwater upconing caused by preferential discharge through boils is expected to involve groundwater flow in the aquifer towards the source vent of the boil, which occurs as a localized point at the bottom of the aquitard (Fig. 1a). It is therefore comparable to saltwater upconing induced by the extraction of fresh groundwater overlying saltwater using partially penetrating wells, which has been described extensively in the literature (e.g. Dagan and Bear, 1968; Reilly and Goodman, 1987; Werner et al., 2012). Upconing from pumping can create a saltwater cone that is stable under certain conditions, notwithstanding that eventually, some saltwater is expected to reach the well due to dispersion effects (Reilly and Goodman, 1987; Werner et al., 2012). Stable upconing plumes are convex in shape and only low-salinity groundwater enters the well (i.e. subcritical conditions), whereas unstable upconing plumes become concave and intercept the well, which subsequently discharges a significant proportion of saltwater (i.e. under critical or supercritical conditions) (Werner et al., 2012). Only a few studies have focused on the behavior of salt plumes that intercept the point of extraction, such as the well screen (e.g. Reilly and Goodman, 1987), possibly because it is the objective of most management strategies to avoid this condition (Werner et al., 2009). Most of the boils observed by De Louw et al. (2010) discharge considerable salt loads, and hence natural saltwater upconing caused by boils most likely occurs under unstable, supercritical conditions.

Generally, two methods are employed in solving the saltwater upconing problem (Bower et al., 1999): the sharp-interface approach and the dispersive solute transport approach. The sharp-interface approach assumes that saltwater and freshwater are immiscible, i.e. separated by an abrupt interface. Mixing is allowed in the dispersive solute transport approach and a dispersive mixing zone between the two fluids is considered. This method represents a more realistic situation, although it is more complex to solve and requires the application of numerical methods (e.g. Diersch et al., 1984; Reilly and Goodman, 1987; Zhou et al., 2005), whereas the sharp-interface approach has been solved using both numerical and analytical methods (e.g. Dagan and Bear, 1968; Zhang et al., 1997; Bower et al., 1999). Saltwater upconing has also been studied using laboratory experiments (e.g. Johannsen et al., 2002; Wer-

ner et al., 2009). However, real-world field data pertaining to saltwater upconing are scarce because of the challenges of undertaking field-based measurements of dynamic salt transport near pumping wells (Jakovovic et al., 2011).

The intent of this study was to examine key features of natural upconing mechanisms associated with boil discharge in Dutch polders. The following aspects were assessed: (i) sources (depths) of boil water and relationships between boil salinity and boil source depths, (ii) the influence of the regional aquifer salinity distribution on upconing, (iii) interactions between boils in boil clusters, and (iv) the effect of regional lateral flow on upconing processes. A combination of field observations and conceptual model testing using numerical simulations was adopted. Two field situations involving saline boils were investigated to provide observations of natural saltwater upconing, and to constrain numerical models in aspects relating to geometry, salinity, boil discharge, aquifer hydraulic heads and hydraulic properties. Numerical modeling and sensitivity analyses were used to explore the influence of different parameters on upconing processes.

2. Study area

Field measurements were carried out in two deep polders in the west of The Netherlands: the Haarlemmermeer Polder and the Noordplas Polder (Fig. 2a). These polders were reclaimed from lakes in different stages between 1750 and 1850. Field site A is in the southwest of the Haarlemmermeer Polder and site B is in the north of Noordplas Polder (Fig. 2a). The ground levels at sites A and B are 5.5 m and 4.7 m below MSL, respectively. The hydrogeology of both sites is similar, and is comparable with many other Dutch deep polders. The upper 6–7 m of the subsurface is an aquitard that consists of clay and peat, in which the boils have developed, and overlying a 30–50 m thick sandy aquifer (Fig. 1). The aquifer hydraulic heads are permanently above ground level at both sites (De Louw et al., 2010; Oude Essink et al., 2010). At study site A, two boils, 4 m apart, were evident as small vents at the ground surface (Fig. 2b). The boils at site B occurred underwater in a ditch, and their outflow vents were not directly visible due to vegetation and turbid water (Fig. 1e). However, at least three outflow vents within an area of 10 m × 2 m could be detected using temperature measurements (De Louw et al., 2010) and by observations of upwelling water and methane (Fig. 1c).

The regional groundwater salinity distributions in the aquifer of the two deep polders are mainly the result of the past Holocene transgressions and the reclamation history (Oude Essink, 1996; Post, 2004; Vos and Zeiler, 2008). Salinization of the aquifer occurred by free convection of seawater mixed with river water during the major transgression between 7500 and 4750 BP. The subsequent development of sand banks and dunes isolated the area from the sea, and fresh rainwater recharged the upper part of the aquifer, displacing the saline groundwater. The construction of the deep polders subsequently changed regional groundwater flow direction and created complex salinity patterns, characterized by large transition zones and a wide range of salinities. The groundwater in the upper 5–10 m of the sandy aquifer of both sites is generally fresh to slightly brackish (Cl concentrations of 0.05–1 g L^{-1}), and salinity gradually increases with depth to Cl concentrations of 3–8 g L^{-1} at 15–40 m below the aquitard (Van Rees Vellinga et al., 1981; De Louw et al., 2010; Oude Essink et al., 2010).

3. Methodology

3.1. Monitoring network

Fig. 2b shows the general set up of the monitoring network around the boil area of site A. Site B had a similar monitoring network configuration. Piezometers with a 0.5 m long screen were installed at 7–8 m below the ground surface and at different distances from the boils (i.e. at 2, 10, 25 and 75 m from boil 1, Fig. 2b), such that they penetrated the top of the sandy aquifer just below the aquitard. Aquifer hydraulic heads were measured in the piezometers for a period of 2.5 years (January 2009–July 2011), with a 1-h frequency using automated pressure loggers (CTD-divers from Schlumberger Water Service®). Measured heads were converted to equivalent freshwater heads using the equations presented in Post et al. (2007). Groundwater was sampled once (18 July 2009) from the piezometers and analyzed for Cl.

Electrical cone penetration tests (ECPT) were carried out to obtain continuous soil electrical conductivity (EC_{bulk}) profiles to a depth of 25 m, and at similar locations to the piezometers. The ECPT measurements were used to map the groundwater salinity distribution in the aquifer to characterize salinity plumes associated with the natural saltwater upconing caused by boils. During penetration, the cone sleeve and tip friction were also measured

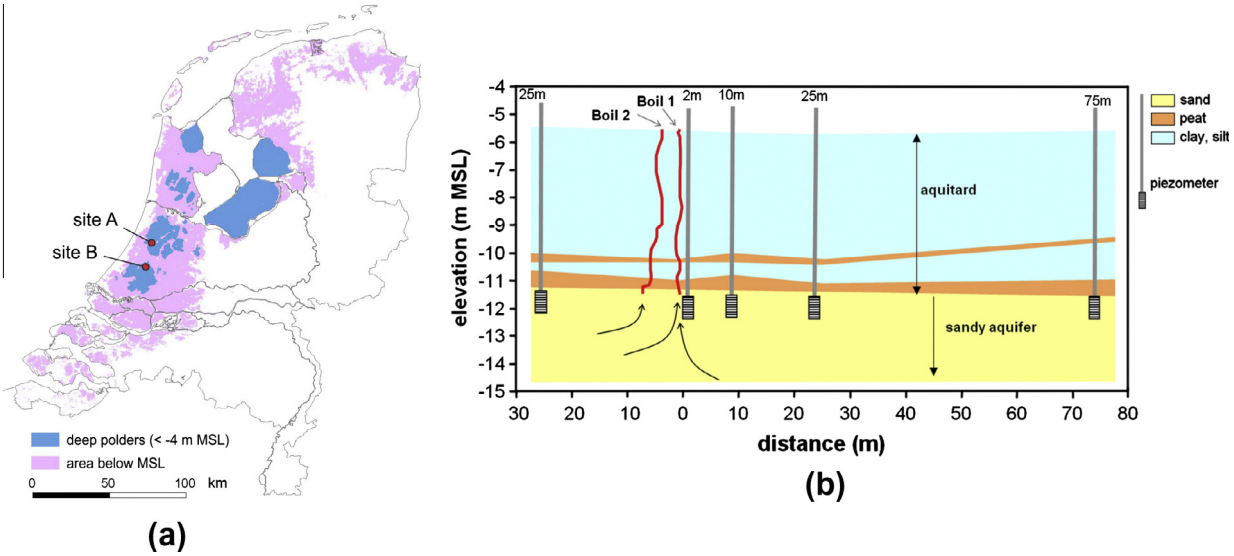

Fig. 2. (a) Location of study site A (Haarlemmermeer Polder) and site B (Noordplas Polder) and (b) general set up of the monitoring network around the boils of site A.

to provide insight into the lithological composition. To obtain the electrical conductivity of water (EC), EC_{bulk} must be multiplied by the formation factor, which depends on the lithology (e.g. Archie, 1942; Friedman, 2005). The cone sleeve and tip friction measurements in the aquifer showed a relative homogeneous composition of medium-coarse sand, for which a formation factor of 4 applies (Goes et al., 2009). Cl concentrations (g L^{-1}) were calculated from the EC (mS cm^{-1}) using the linear relation derived by De Louw et al. (2011b): $Cl = 0.36EC - 0.45$ (valid for ECs > 1.25 mS cm^{-1}). The discharge and EC of the two boils at site A were measured manually by directly collecting the outflowing boil water in a measuring cup. The discharge and EC were measured weekly for a period of 1.5 years. As the outflow vents of the boils at site B were underwater, the boil fluxes and ECs could not be easily measured. The boil salinity at site B was measured once by isolating the boil using a collection vessel.

The possibility of sealing the boils as a measure to abate salinization was examined. Expanding and persisting fluids were injected in the aquifer near the source vent in an attempt to seal the boil. These subsequently flowed towards the source vent due to the flow created by the boil. While these field experiments are not described in detail in this article, the observed changes in the groundwater system and boil characteristics due to the sudden drop in or cessation of boil discharge (Q_{boil}) are included in the analysis. The boil sealing attempts were carried out on 27th May 2011 at site A and 17th September 2009 at site B.

3.2. Numerical modeling of saltwater upconing

3.2.1. Modeling approach

The objective of the modeling was to provide a framework to better understand the field observations and to undertake sensitivity analyses to evaluate the different parameters influencing upconing. The simulated situation was a homogeneous, anisotropic confined aquifer, with each boil represented by a point extraction at the aquifer top. Consequently, the overlying aquitard (and complex, rapid flows through it) was neglected, and the focus was on groundwater flow and saltwater upconing in the aquifer. The simulation of aquitard flow would require the model to predict preferential flow through boil conduits (Fig. 1), which are difficult to accurately represent using existing variable-density transport codes. Estimated flow velocities in boils were as high as 800 m d^{-1} (De Louw et al., 2010), and the associated travel times of water flowing through the conduits in the order of minutes. Given that the flow processes and temporal and spatial scales for aquitard flow are in contrast to those associated with upconing, conduit flow through the aquitard was not considered. Instead, the boil source vents were simulated as point sinks in the model, because the focus of the paper was aquifer flow and transport processes induced by boil discharge. The models are highly idealized accounts of typical conditions encountered in Dutch deep polders. We intentionally avoid calibration, partly because aquifer parameter distributions and the long-term temporal behavior at specific sites are not well constrained, but also to allow us to examine simplified situations and develop general intuition about boil-induced upconing processes.

The variable-density flow and transport code SEAWAT version 4 (Langevin et al., 2007) was used. Flow and transport may be considered in an axisymmetric domain when a single boil is considered and regional flow is neglected. The parameters of SEAWAT were modified to represent radial flow and transport, reducing the governing equations by one dimension and improving the efficiency of model computations (Langevin, 2008). Fully 3D models were used to incorporate multiple boils and regional flow effects.

3.2.2. Reference case

A reference case was defined and parameterized based on hydrogeological data of The Netherlands (REGIS II, 2005) and aquifer properties, salinity distributions and boil characteristics for the Noordplas Polder (measured by De Louw et al. (2010)) and for sites A and B. The parameter values of the reference case are summarized in Table 1. The reference case was intended to develop conceptual intuition of functional relationships for idealized conditions, and hence comprises reduced complexity relative to real-world situations. For example, the axisymmetric flow conditions of the reference case preclude the analysis of multiple boils or regional flow effects, which are encountered in field conditions. Regional flow and multiple boils were examined with the more computationally demanding 3D models.

A single-boil entry vent was simulated as a point sink at the top of a 50-m thick (D) homogeneous, anisotropic confined aquifer, with a porosity (n) of 0.30, a horizontal hydraulic conductivity (K_h) of 20 m d^{-1} and a vertical hydraulic conductivity (K_v) of 6.67 m d^{-1} (i.e. anisotropy of 3) (Fig. 3). A constant extraction rate (Q_{boil}) of 30 m^3 d^{-1} was adopted, which falls within the range of 0.5–100 m^3 d^{-1} for measured single-boil fluxes (De Louw et al., 2010). Transient simulations for a period of 100 years were undertaken to explore the evolution of upconing following the creation of a new boil. One stress period of 100 years was subdivided in 10,000 flow time steps of 3.65 days. Each flow time step was automatically divided into a number of transport time steps according to the stability criterion Courant number, which was not allowed to be greater than 1 (Langevin et al., 2007).

The initial aquifer salinity distribution applied in the models corresponds to the regional aquifer salinity distribution in the absence of boils, and is shown in Fig. 3. The fresh groundwater above the transition zone was assigned a Cl concentration (Cl_f) of 0 g L^{-1} with a density (ρ_f) of 1000 kg m^{-3}. For the saline groundwater below the transition zone, a Cl concentration (Cl_s) of 5 g L^{-1} with a density (ρ_s) of 1006.6 kg m^{-3}, a typical value for the aquifers at sites A and B, was adopted. These correspond with a relative density difference ($\beta = (\rho_s - \rho_f)/\rho_f$) equal to 0.0066. The density varied linearly with the Cl concentration because the saline groundwater bodies in the Dutch subsurface are mixtures of seawater (ρ_s = 1025 kg m^{-3}; Cl_s = 19 g L^{-1}), and freshwater (ρ_f = 1000 kg m^{-3}; Cl_f = 0 g L^{-1}). De Louw et al. (2011b) showed that freshwater–saltwater transition zones in Dutch aquifers can be well described by the spatial moments method. With this method, the derivative of the salinity profile is described by a normal distribution function, from which the centre of mass (1st moment) indicates the centre of the transition zone C_{if} (Fig. 3). The Cl concentration at the initial C_{if} position is $0.5Cl_s$. The location of C_{if} was assumed to occur at the position of $0.5Cl_s$, obtained from modeled salinity distributions. The variance (2nd moment) is a measure of the extent of the transition zone. Five times the standard deviation was used to characterize the initial width of the transition zone (W_{if}), which equals the thickness between salinities of $0.01Cl_s$ and $0.99Cl_s$ (Fig. 3b). The initial position of C_{if} was set at 15 m depth and the initial W_{if} was 15 m, which corresponds with the average conditions in the aquifers at sites A and B (Fig. 3).

The reference case was simulated in both axisymmetric and 3D domains for the purposes of comparison. SEAWAT can be manipulated to simulate an axisymmetric geometry by using a grid of one row, l columns and m layers, and adjusting the input parameters to account for the increase in flow area with radial distance (r) (Langevin, 2008). That is, n, K_h, K_v and specific storage (S_s) were scaled by $2\pi r$. The axisymmetric domain was 1500 m long and was represented by 55 variable-spaced columns, with a cell width of 0.5 m at the boil increasing to 50 m at an r of 1000 m (Fig. 3). The vertical extent was divided into 50 model layers, using thicknesses of 0.5 m (upper 10 m), 1.0 m (10–20 m depth) and 1.5 m (20–50 m

Table 1
Parameter values of the reference case and different upconing cases. The parameter values of the reference case are listed under 'Ref'. An upconing case is defined by a 'Nr' and a character 'a', 'b', 'c' or 'd'. Each upconing case differs from the reference case by only one or two parameters for which the values are listed under 'a', 'b', 'c' or 'd'.

Category	Nr	Parameter	Unit	Type of model	a	b	Ref.	c	d
Boil discharge	1	Q_{boil}	$m^3\ d^{-1}$	Axi	5	15	30	50	100
Hydrogeology	2	K_h	$m\ d^{-1}$	Axi	5	10	20	40	60
		K_v	$m\ d^{-1}$		1.7	3.3	6.7	13.3	20
	3	K_h	$m\ d^{-1}$	Axi	5	10	20	40	60
		K_v	$m\ d^{-1}$		6.7	6.7	6.7	6.7	6.7
	4	K_h	$m\ d^{-1}$	Axi	20	20	20	20	20
		K_v	$m\ d^{-1}$		2.2	3.3	6.7	13.3	26.7
	5	D	m	Axi	25	35	50	75	100
	6	n	–	Axi	0.20	0.25	0.30	0.35	0.45
Dispersivity	7	α_L	m	Axi	0	0.05	0.10	0.50	1
		α_T	m		0	0.005	0.01	0.05	0.1
	8	α_L	m	Axi	0.01	0.05	0.10	0.50	1
		α_T	m		0.01	0.01	0.01	0.01	0.01
	9	α_L	m	Axi	0.10	0.10	0.10	0.10	0.10
		α_T	m		0.10	0.02	0.01	0.002	0.001
Aquifer salinity distribution	10	C_{if}	m	Axi	5	10	15	20	30
	11	W_{if}	m	Axi	0	10	15	20	30
	12	Cl_s	$g\ L^{-1}$	Axi	1	2.5	5	10	19
		β	–		0.0013	0.0033	0.0066	0.0132	0.0250
Regional flow	13	$\Delta h/\Delta x$	–	3D	0.0001	0.0002	0.0000	0.0003	0.0005
Multiple boils	14	Boil config.	–	3D	A[a]	B[b]	1 Boil	C[c]	

[a] Boil configuration (A) 3 boils at 2 m distance from each other, Q_{boil} are 18, 10 and 2 $m^3\ d^{-1}$.
[b] Boil configuration (B) 3 boils at 2 m distance from each other, Q_{boil} are 14, 2 and 14 $m^3\ d^{-1}$.
[c] Boil configuration (C) 2 boils at 7 m distance from each other, Q_{boil} are 15 and 15 $m^3\ d^{-1}$.

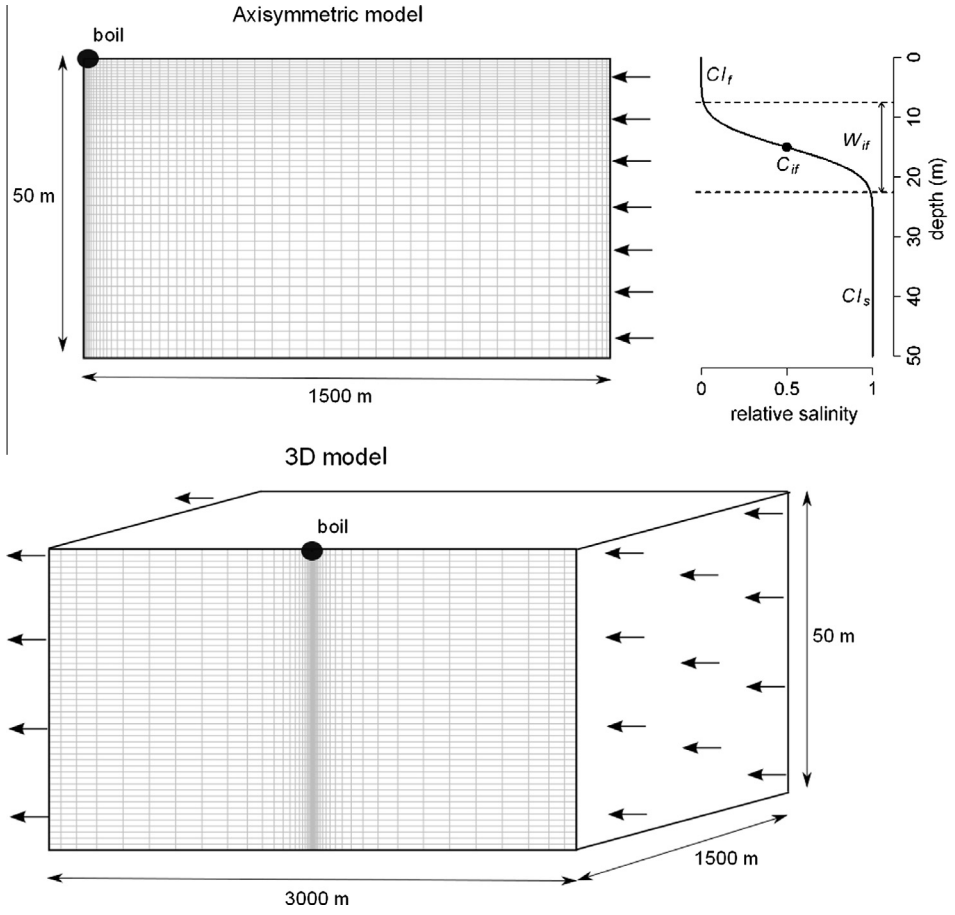

Fig. 3. General set up of the axisymmetric and 3D-models (situation with lateral regional groundwater flow is shown) and the aquifer salinity depth distribution adopted into the models as initial condition and applied to groundwater flowing into the model domain. All model boundaries are no-flow and no-mass flux boundaries except those indicated with arrows which are specified-head boundaries.

depth). Specified-head boundary conditions representing density-corrected hydrostatic conditions were adopted at a distance of 1500 m from the boil. The specified-head boundaries were assigned a constant salt concentration according to the regional aquifer salinity distribution shown in Fig. 3. The top and bottom of the aquifer were no-flow and no-mass flux boundaries.

The total domain of the 3D model was cut in half along the symmetry axis to reduce calculation times, leading to a domain size of 3000 m in length by 1500 m in width (Fig. 3). The boil was placed at the middle of the symmetry boundary so that the side boundaries were at least 1500 m from the boil. The symmetry boundary was considered as a no-flow boundary. Otherwise, the same boundary conditions were applied as for the axisymmetric model. Applying the same cell sizes for 3D models as adopted in the axisymmetric models resulted in extremely long calculation times (>20 days), and this restricted the cell sizes to larger than that used for the axisymmetric model. The model domain of 3000 m by 1500 m was therefore divided into 57 columns and 29 rows. A minimum cell width in the horizontal plane of 1 m was used near the boil, and this increased by a factor of 1.3 to a maximum cell width of 150 m. A thickness of 1 m was adopted for all 50 model layers.

3.2.3. Upconing cases

In total, 56 upconing cases were assessed in undertaking sensitivity analyses. A range of hydraulic and solute transport parameters, representing idealized conditions, typical of the field sites and Dutch deep polders more generally (Table 1), were adopted. Each upconing case differed from the reference case by modification of only one or two parameters. Parameters were modified according to the following categories (Table 1): Q_{boil}, hydrogeological properties of the confined aquifer (K_h, K_v, D, n), dispersivity (α_L, α_T), aquifer salinity distribution (C_{if}, W_{if}, β), number of boils, and regional flow. Regional flow was introduced in 3D models by modifying the specified-head boundaries normal to the symmetry boundary to control the regional hydraulic gradient and by adopting no-flow conditions to the boundary opposite to the symmetry boundary (Fig. 3). Regional hydraulic gradients ranged from 0.0001 to 0.0005 (see Table 1). For the multiple boil cases, three different boil configurations (A, B and C, Table 1) were simulated. The boils were placed in a line at the symmetry boundary of the 3D model, in a corresponding manner to several field situations where multiple boils occur in or along straight ditches (De Louw et al., 2010). The total Q_{boil} in multiple boil simulations was equal to the single Q_{boil} of the reference case.

3.2.4. Model output analysis

The model output analysis involved different aspects of saltwater upconing, including boil salinity, distributions of drawdown and transition zone characteristics (C_{if} and W_{if}), and the sources of boil water. The results of the reference case were compared qualitatively with the field observations of sites A and B to verify that the conceptual model is a reasonable surrogate for typical boil-induced upconing below Dutch polders. Further, the reference case was compared to the results of a simulation without density effects, in which the salt acts as a conservative tracer, to evaluate the mixed convective processes associated with upconing mechanisms, and to explore differences in upconing that might otherwise occur in regions where aquifer salinity contrasts are lower or absent (e.g. in the Nieuwkoop Polder and parts of Noordplas Polder, Haarlemmermeer Polder and Zuidplas Polder; Van Rees Vellinga et al., 1981).

Streamlines and travel times were calculated by 50 forward-tracking particles placed at 1400 m from the boil and equally distributed with depth, using the post-processing package MODPATH version 3 (Pollock, 1994). The vertical variation in groundwater flow rates was assessed to identify the respective depth-contributions to Q_{boil} thereby offering insights into the sources of boil water. For the axisymmetric and 3D models without regional flow, the contributing depths can be determined from the calculated horizontal flow rates away from the boil (>200 m), where vertical flow velocities are small compared to horizontal flow velocities. The contribution of different depths to Q_{boil} is given as CD_i, where CD_i is the fraction of the total discharge occurring across a depth interval i. Since CD_i represents the sources of boil water, the multiplication of CD_i with the regional aquifer salinity distribution (Cl_i) for an aquifer of thickness D should result in the boil salinity, as shown by the following:

$$\text{boil salinity} = \sum_{i=m}^{i=1} CD_i \cdot Cl_i \quad (1)$$

With m the number of layers of thickness D/m. Eq. (1) assumes steady-state conditions and neglects dispersion effects.

4. Results

4.1. Monitoring results

Fig. 4a and b shows the measured Q_{boil} and Cl concentrations for site A, during the period 20 April 2011–20 June 2012, which included a boil sealing attempt. Prior to the boil sealing attempt, boil 1 produced an average discharge of 16.5 $m^3\ d^{-1}$ and an average Cl concentration of 2.6 $g\ L^{-1}$. For the same period, the average discharge of boil 2 was only 0.7 $m^3\ d^{-1}$ and the average Cl concentration was lower, namely 0.9 $g\ L^{-1}$.

The in situ groundwater salinity was determined from ECPT measurements at site A. Fig. 4c shows the ECPT-based isochlors of Cl concentrations of 0.5 $g\ L^{-1}$, 1.0 $g\ L^{-1}$, and 2.5 $g\ L^{-1}$ in cross section, together with the direct measurements of Cl in piezometers and of boil discharge (boil 1). Saltwater upconing towards the boil is clearly visible in the aquifer. At 75 m from the boil, a Cl concentration of 2.5 $g\ L^{-1}$ is found at 15 m below the aquitard, whereas the same Cl concentration is found 2 m from the boil at 6 m below the aquitard. The 9 m difference in the 2.5 $g\ L^{-1}$ isochlor is attributed to boil discharge effects. Groundwater Cl concentrations just below the aquitard were 0.39 $g\ L^{-1}$ at 75 m, 0.41 $g\ L^{-1}$ at 25 m and 0.76 $g\ L^{-1}$ at 2 m from boil 1. The boil water Cl concentration was 2.6 $g\ L^{-1}$, which is more than three times the Cl concentration of groundwater just below the aquitard at only 2 m from the boil. This illustrates that the boil caused saltwater upconing in the form of steep salinity isochlors (Fig. 4c). At site B, the observed upconing was similarly localized and steep. Site B boil water had a Cl concentration of 1.1 $g\ L^{-1}$, and the groundwater in the upper aquifer at 2 m from the boil had a Cl concentration of 0.6 $g\ L^{-1}$.

Fig. 4d illustrates the decreasing trend (towards boil 1) in the equivalent freshwater heads. The head measured at 2 m from boil 1 was about 8 cm lower than at 25 m from the boil, and was about 11 cm lower than at 75 m from the boil. For site B, a similar decreasing trend in the aquifer hydraulic head towards the boil was observed, with a 10 cm lower head at 2 m than at 25 m from the boil. The heads at 25 m and 75 m from the boil were similar (within ±2 cm). The observed decreasing trends in the aquifer hydraulic heads towards the boil areas of sites A and B are assumed to be the boils' drawdown cone.

Some noteworthy observations were made during the boil sealing experiment. First, the sudden cessation of groundwater discharge caused by sealing the boil 1 vent at site A caused a rapid increase in aquifer hydraulic head of 0.12 m at 2 m from the sealed boil. No head increase was observed at the other piezometers at larger distances from the boil. Second, the discharge of boil 2 doubled as a result of the boil 1 sealing attempt and the associated in-

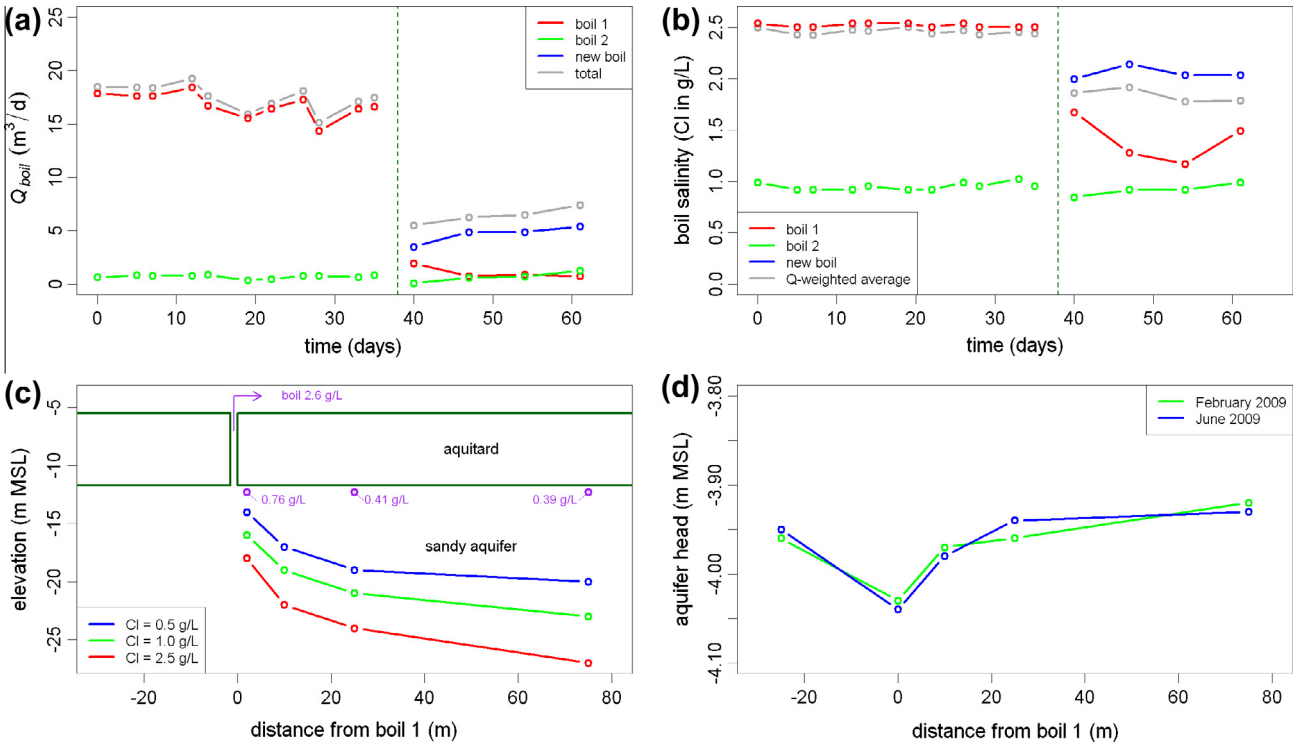

Fig. 4. Field measurements of boil site A. (a) Q_{boil} and (b) boil salinity with time; the boil sealing experiment is indicated by the dotted green lines, (c) isochlors of Cl concentration from ECPT measurements and groundwater Cl concentration (in purple), and (d) equivalent freshwater aquifer heads. (For interpretation of the references to color in this figure legend, the reader is referred to the web version of this article.)

creased aquifer hydraulic head. Third, by sealing off both boils 1 and 2, a new boil developed at the surface at 4 m distance from boil 2 with a discharge of about 5 $m^3\ d^{-1}$ and a Cl concentration of about 2 $g\ L^{-1}$ (Fig. 4a and b).

4.2. Reference case modeling

The simulation results of the axisymmetric reference case are shown in Fig. 5 as solid lines. The boil water salinity increased sharply to $0.20Cl_s$ in the first 15 years, and then increased gradually to $0.32Cl_s$ by 100 years, when it still did not reach a steady-state condition (Fig. 5a). Similarly, the aquifer hydraulic head drawdown (Fig. 5b) and the groundwater salinity distribution (characterized by C_{if} and W_{if}; Fig. 5e and f), did not reach steady state after 100 years. The drawdown at the top of the aquifer rapidly decreased with distance (Fig. 5b and c) and with depth (Fig. 5c). The drawdown was 0.95 m at the boil vent, 0.20 m at 2 m from the boil and 0.05 m at 39 m from the boil. Fig. 5d and f shows that W_{if} decreased towards the boil. This is caused by the convergence of streamlines as shown in Fig. 6a. The streamline and travel time distributions showed that groundwater flows faster above than below C_{if} (Fig. 6a). The contributing depth distribution (given by CD_i) showed an inverse relationship with the aquifer salinity distribution (Fig. 7a). That is, the boil extracted more low-salinity groundwater per m aquifer from above C_{if} than high-salinity groundwater from below C_{if}. The fraction of Q_{boil} originating from above C_{if} is referred to here as the shallow contribution (CD_{sh}), which was 0.72 for the reference case.

The differences between the results of the axisymmetric and 3D forms of the reference case model were small. The boil salinity breakthrough curve of the 3D reference model is plotted in Fig. 5a, showing slightly higher (i.e. by 3% after 100 years) boil salinity than the axisymmetric reference case. For all other aspects of upconing shown in Fig. 5 (drawdown, upconing of salinity contours, C_{if} and W_{if}), the 3D model produced similar (<1% error) results to the axisymmetric model, and these are therefore not shown in Fig. 5b–f.

4.3. Axisymmetric upconing scenarios

Axisymmetric upconing scenarios allowed for the assessment of several factors influencing boil-induced upconing, such as: boil discharge, the regional aquifer salinity (density) distribution (i.e. the specified salinity profile at model boundaries), aquifer properties such as K_h, K_v, D, n and dispersivity. Model results after 100 years are summarized in Tables 2–4.

Q_{boil} had a major impact on all aspects of saltwater upconing (Tables 2–4). A low discharge rate of 5 $m^3\ d^{-1}$ caused a small drawdown cone (drawdown of 0.05 m at 2 m from the boil and at 1.2 m depth; Table 2, case 1a). In this case, about 90% of the boil water came from above the C_{if} resulting in a boil salinity of $0.05Cl_s$. (Table 4) With a high Q_{boil} of 100 $m^3\ d^{-1}$(case 1d), some 60% of the boil water came from below the C_{if}, leading to a boil salinity of $0.63Cl_s$. Thus, higher discharge rates resulted in more boil water coming from below the C_{if}, and therefore higher boil salinities (Fig. 8), as expected (Reilly and Goodman, 1987; Ma et al., 1997).

The regional aquifer salinity distribution, characterized by C_{if}, W_{if} and β, had also a major impact on all aspects of upconing (Tables 2–4). Upconing was most sensitive to changes in β and C_{if}, whereas W_{if} was of lesser importance (Fig. 8). The significance of the regional aquifer salinity (or density) distribution is clearest in the contributing depth distributions, which show a similar but opposite form to the regional aquifer salinity distribution (Fig. 7a–c). As expected, a deeper C_{if} resulted in a larger CD_{sh}, resulting in lower boil salinities (Table 4; cases 10a–d). Fig. 7a clearly shows that the contributing depth distribution was modified significantly by density effects; a larger β led to a higher CD_{sh} which resulted in lower relative boil salinities (Table 4; cases 12a–

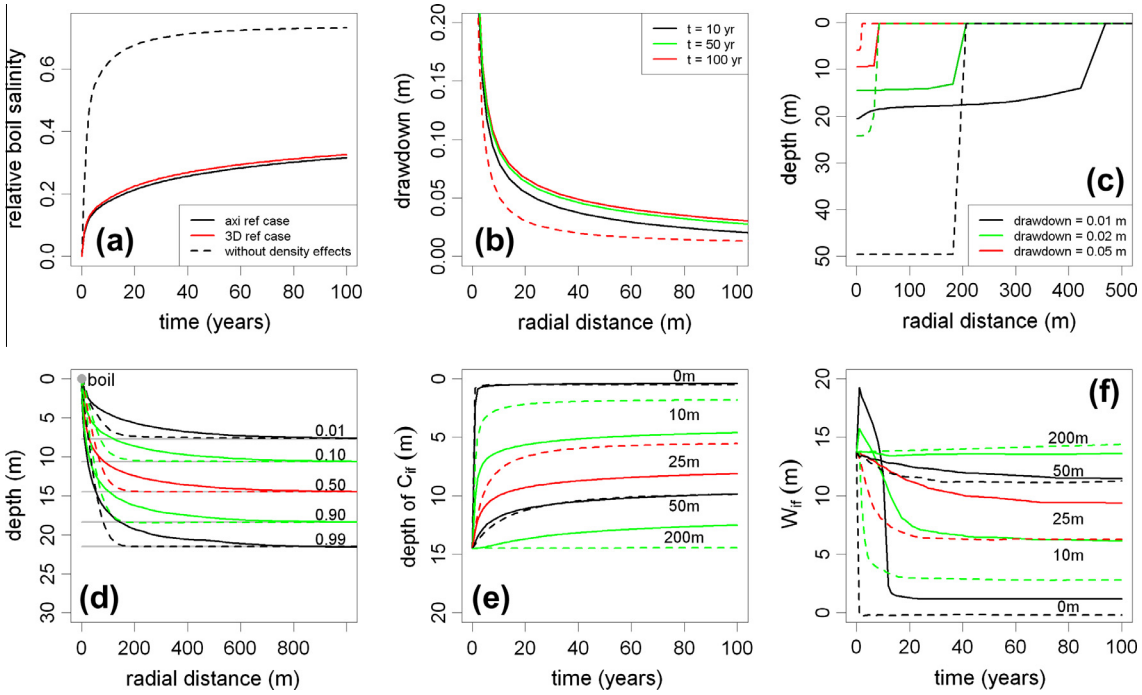

Fig. 5. Model results of axisymmetric reference case with density effects (full lines) and without density effects (dotted lines): (a) boil salinity with time, (b) freshwater head drawdown for different simulation times, (c) freshwater head drawdown contours (after 100 years), (d) upconing of different relative salinity contours (after 100 years); grey lines indicate the initial position of the salinity contours, and (e) change of C_{if} and (f) W_{if} with time at different distance from the boil.

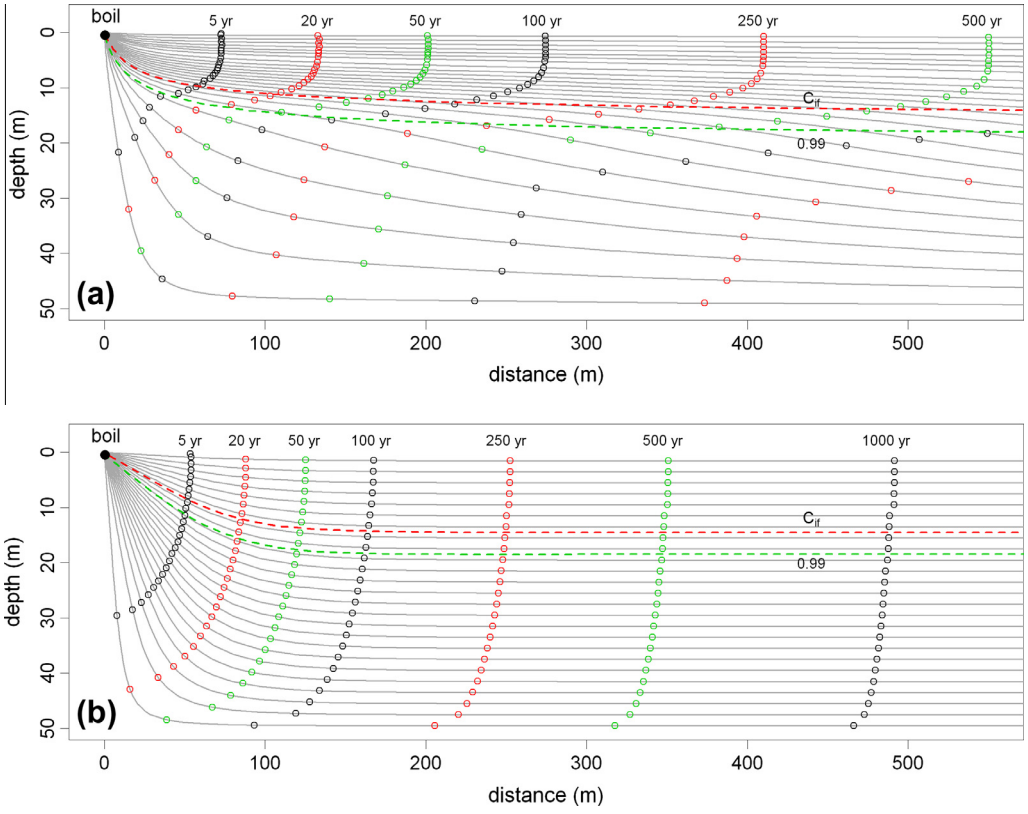

Fig. 6. Streamlines towards the boil with travel times to the boil (in years) for the reference case (a) with density effects and (b) without density effects. The relative salinity contours of 0.50 (C_{if}) and 0.99 (bottom transition zone) are indicated as well. The forward calculated streamlines are based on the flow velocity field after a simulation time of 100 years. The colored points at the streamlines indicate the travel time to the boil. (For interpretation of the references to color in this figure legend, the reader is referred to the web version of this article.)

d). This illustrates the stabilizing effect of the denser saltwater on upconing, as expected (e.g. Dagan and Bear, 1968; Reilly and Goodman, 1987; Jakovovic et al., 2011). Neglecting density variations in the aquifer and presuming that salt acts merely as a conservative

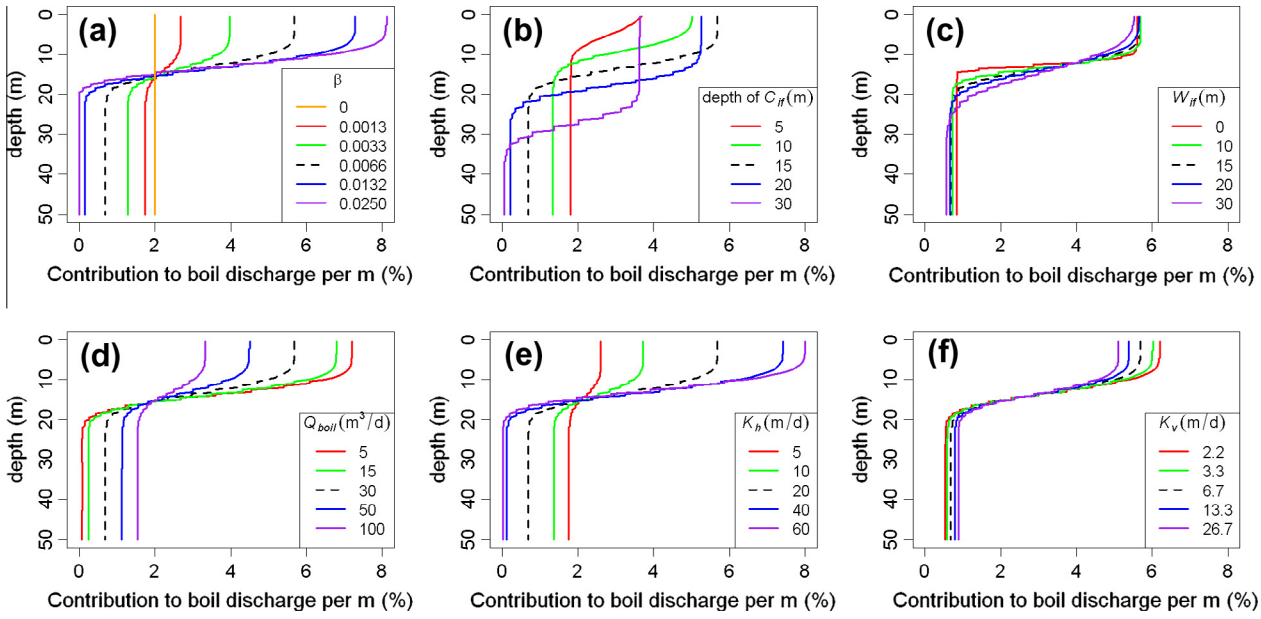

Fig. 7. Contributing depth distribution (at T = 100 years) for various upconing cases defined in Table 1: (a) β; (b) depth of C_{if}; (c) W_{if}; (d) Q_{boil}; (e) K_h; (f) K_v. The colored lines refer to the different upconing cases listed Table 1 and the black dotted lines show the reference case. (For interpretation of the references to color in this figure legend, the reader is referred to the web version of this article.)

tracer, resulted in the lowest CD_{sh} (0.30) and the highest relative boil salinity ($0.73Cl_s$) of all simulated cases (except case 10a). In contrast to the density-dependent simulated cases, the density-independent simulation show that travel times were almost equally distributed over depth (Fig. 6a) and boil water came from all depths in virtually equal amounts (Fig. 7a). Both the drawdown and saltwater cone were steeper and more localized (i.e. smaller lateral extent) without density effects (Fig. 5c and d). The density-independent simulation reached steady-state conditions more rapidly, i.e. drawdowns stabilized within 1 year and both boil salinity and the salinity distribution in the aquifer remained constant after 73 years.

K_h had a large impact on all aspects of the natural saltwater upconing mechanism. Larger K_h led to smaller drawdown and saltwater cones, both in height and lateral extent, and lower boil salinities due to larger contributions of shallow, fresher groundwater (Tables 2–4). The effect of K_h is clearly visible in the contributing depth distribution (Fig. 7e). Effects of K_v were much smaller but opposite to the effect of K_h concerning contributing depths (Fig. 7f) and boil salinity (Fig. 8). The difference in effect between K_h and K_v on pumping water salinity was also found through numerical simulations by Ma et al. (1997). D had a relatively minor effect on upconing processes. That is, boil salinities were virtually the same ($0.32Cl_s$) for D values of 50, 75 and 100 m, but noticeably lower for D values smaller than the reference case, i.e. $0.29Cl_s$ for D = 35 m and $0.26Cl_s$ for D = 25 m (Fig. 8).

The longitudinal (α_L) and transverse dispersivity (α_T) did not have a significant effect on drawdown (Table 2). In agreement with others (e.g. Reilly and Goodman, 1987; Zhou et al., 2005), α_T affected W_{if}, whereas the impact of α_L was negligible (Table 3). Larger values of α_T than those used for the reference case resulted in thicker W_{if}, smaller CD_{sh}, and higher boil salinities (Tables 3 and 4).

Table 2
Model results of the different upconing cases defined in Table 1, showing the distance from the boil and depth below the boil of the 0.05 m drawdown contour after 100 years of simulation.

Category	Nr	Parameter	Distance of 0.05 m drawdown (m)					Depth of 0.05 m drawdown (m)				
			a	b	Ref.	c	d	a	b	Ref.	c	d
Boil discharge	1	Q_{boil}	2	11	39	73	165	1	6	9	12	29
Hydrogeology	2	K_h, K_v	177	73	39	12	6	50	14	9	6	3
	3	K_h, $K_v = c$	159	73	39	15	9	50	14	9	6	3
	4	K_v, $K_h = c$	49	45	39	33	28	9	9	9	10	10
	5	D	44	41	39	37	36	10	10	9	9	9
	6	n	41	40	39	38	38	9	9	9	9	9
Dispersivity	7	α_L, α_T	39	39	39	38	38	9	9	9	9	9
	8	α_L, $\alpha_T = c$	39	39	39	39	39	9	9	9	9	9
	9	α_T, $\alpha_L = c$	39	38	39	39	39	9	9	9	9	9
Aquifer salinity	10	C_{if}	19	31	39	31	17	6	7	9	11	10
Distribution	11	W_{if}	38	39	39	38	36	9	10	9	9	10
	12	β	14	21	39	66	97	7	8	9	10	11
Regional flow	13	$\Delta h/\Delta x$	42	40	39	38	35	10	10	9	10	10
Multiple boils	14		38	39	39	39		9	9	9	9	

c = constant.

Table 3
Model results of the different upconing cases defined in Table 1, showing the centre depth (C_{if}) and width (W_{if}) of the transition zone at 25 m from the boil after 100 years of simulation.

Category	Nr	Parameter	C_{if} (m below top aquifer)					W_{if} (m)				
			a	b	Ref.	c	d	a	b	Ref.	c	d
Boil discharge	1	Q_{boil}	13	9	7	6	5	16	16	9	7	7
Hydrogeology	2	K_h, K_v	5	7	7	9	10	7	8	9	16	17
	3	K_h, $K_v = c$	7	7	7	8	9	9	8	9	17	18
	4	K_v, $K_h = c$	6	7	7	8	8	8	8	9	9	9
	5	D	8	8	7	7	7	10	9	9	8	8
	6	n	7	7	7	7	7	8	8	9	9	9
Dispersivity	7	α_L, α_T	7	7	7	8	8	7	8	9	15	26
	8	α_L, $\alpha_T = c$	7	7	7	7	7	9	9	9	9	9
	9	α_T, $\alpha_L = c$	8	7	7	7	7	25	10	9	7	7
Aquifer salinity	10	C_{if}	2	4	7	12	26	7	8	9	17	24
Distribution	11	W_{if}	7	7	7	7	7	5	7	9	11	17
	12	β	5	6	7	9	11	7	7	9	16	17
Regional flow	13	$\Delta h/\Delta x$	8	8	7	9	10	12	16	9	19	25
Multiple boils	14		8	7	7	7		8	8	9	8	

c = Constant.

Table 4
Model results of the different upconing cases defined in Table 1, showing the relative boil salinity and the shallow contribution (CD_{sh}) after 100 years of simulation.

Category	Nr	Parameter	Relative boil salinity					Shallow contribution, CD_{sh} (fraction)				
			a	b	Ref.	c	d	a	b	Ref.	c	d
Boil discharge	1	Q_{boil}	0.05	0.12	0.32	0.41	0.63	0.93	0.88	0.73	0.59	0.45
Hydrogeology	2	K_h, K_v	0.59	0.51	0.32	0.13	0.10	0.41	0.51	0.73	0.92	0.96
	3	K_h, $K_v = c$	0.66	0.51	0.32	0.13	0.09	0.38	0.51	0.73	0.93	0.97
	4	K_v, $K_h = c$	0.23	0.25	0.32	0.36	0.44	0.79	0.77	0.73	0.70	0.67
	5	D	0.26	0.29	0.32	0.32	0.32	0.77	0.74	0.73	0.71	0.71
	6	n	0.37	0.31	0.32	0.32	0.32	0.74	0.74	0.73	0.73	0.73
Dispersivity	7	α_L, α_T	0.30	0.31	0.32	0.35	0.42	0.75	0.74	0.73	0.70	0.66
	8	α_L, $\alpha_T = c$	0.32	0.32	0.32	0.33	0.35	0.73	0.73	0.73	0.73	0.73
	9	α_T, $\alpha_L = c$	0.38	0.36	0.32	0.31	0.31	0.67	0.72	0.73	0.74	0.74
Aquifer salinity	10	C_{if}	0.90	0.66	0.32	0.09	0.02	0.17	0.44	0.73	0.92	0.98
Distribution	11	W_{if}	0.29	0.30	0.32	0.37	0.37	0.71	0.74	0.73	0.73	0.71
	12	β	0.67	0.53	0.32	0.13	0.08	0.39	0.54	0.73	0.92	0.98
Regional flow	13	$\Delta h/\Delta x$	0.32	0.31	0.33	0.29	0.27	0.72	0.73	0.70	0.73	0.74
Multiple boils	14		0.31^{dw}	0.31^{dw}	0.33	0.30^{dw}		0.70	0.70	0.70	0.71	

c = Constant; dw = discharge weighted average.

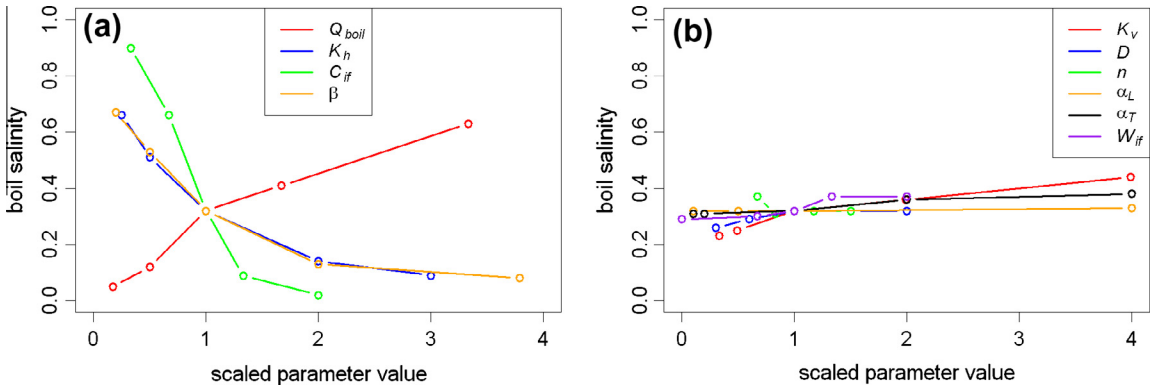

Fig. 8. Spider diagrams of relative boil salinity versus scaled parameter value (relative to the parameter value of the reference case) for the different axisymmetric cases listed in Table 1. Diagram (a) shows the parameters that had a large impact on boil salinity compared to the parameters shown in diagram (b).

4.4. 3D upconing scenarios

Fig. 9 shows results of the 3D simulations of multiple boil cases for three different boil configurations. The calculated salinities of neighboring boils in a boil cluster varied over a wide range for configuration A and B (Fig. 9). For example, the boil salinities after 100 years of the three boils of configuration A were $0.03Cl_s$, $0.23Cl_s$ and $0.37Cl_s$ (Fig. 9). Interestingly, the highest boil salinity

($0.49Cl_s$ after 100 years) was simulated for the boil with the smallest discharge (2 $m^3\ d^{-1}$) (i.e. configuration B in Fig. 9). This boil was positioned between two high-flow boils, which enhanced saltwater upconing to the middle, low-flow boil because the inflow of shallower and fresher groundwater was impeded. The results also showed that extracting the same amount of groundwater but over a larger area led to slightly wider saltwater cones being formed below the boils (Fig. 9). Despite the large differences in boil salinities within a boil configuration, the total salt load was similar for all cases. The largest total Cl load of 49 kg d^{-1} was calculated for the single-boil case, and the smallest Cl load of 45 kg d^{-1} was obtained for configuration C (Fig. 9).

Applying a regional groundwater flow component had a large impact on the groundwater flow pattern (Fig. 10). The streamlines illustrated in Fig. 10 show that sources of boil water are considerably shallower in the presence of a regional gradient typical for Dutch polders. For example, for the case with the smallest regional hydraulic gradient (0.0001; case 13a), the deepest streamline that ended in the boil came from 39 m depth (Fig. 10a and b), whereas for cases without regional flow, the whole aquifer (50 m) contributed to Q_{boil} (Figs. 6 and 7). This streamline divided groundwater flow into a local system with groundwater flow towards the boil and a regional system with groundwater flow bypassing the boil, and is referred to hereafter as the dividing streamline. The dividing streamlines of all four regional flow cases are shown in Fig. 10c, which shows that a larger regional flow component resulted in a shallower position of the dividing streamline. Surprisingly, regional flow had only small impacts on boil salinity, despite significant changes in the groundwater flow patterns. The largest increase in regional flow (gradient change from 0 to 0.0005) caused a decrease in boil salinity from $0.32Cl_s$ to $0.27Cl_s$ (Table 4, cases 13a–d).

5. Discussion

5.1. Comparison of field and modeling results

Several aspects of the field situation were simplified or neglected in the numerical model. For example, characteristics such as the salinity distribution across the entire aquifer thickness, the time since boil development, and regional flow rates were largely unknown for the field situation. Despite this, simulated saltwater upconing and drawdown were largely consistent with the scale of observed values at sites A and B. That is, the model calculated a 9 cm lower head at 2 m than at 75 m from the boil for case 1b (with a Q_{boil} of 15 $m^3\ d^{-1}$; observed Q_{boil} of site A was 17 $m^3\ d^{-1}$), which is of similar magnitude to the observed head difference (11 cm) over the same distance at field site A (Fig. 4d). The simulated position of the $0.5Cl_s$ isochlor (8 m deeper at 75 m than at 2 m from the boil) largely corresponds with the field situation (2.5 g L^{-1} isochlor was 9 m deeper at 75 m than at 2 m from the boil; Fig. 4c).

The small-scale spatial variations in boil salinity within a small area of clustered boils observed at site A were similar to those obtained from the 3D numerical model. Modeling scenarios showed that salinity variations between clustered boils are determined by the combination of the discharge and position of individual boils within a boil area. However, the total combined discharge of the boil cluster is the principal factor that controls both saltwater upconing and total salt loads. As such, boil clusters such as those considered here can be reasonably represented as one point sink if the primary concerns are large-scale upconing and boil contributions to surface water salinization.

The differences in observed boil salinities at site A (Fig. 4b) indicate that the boils are probably not interconnected within the

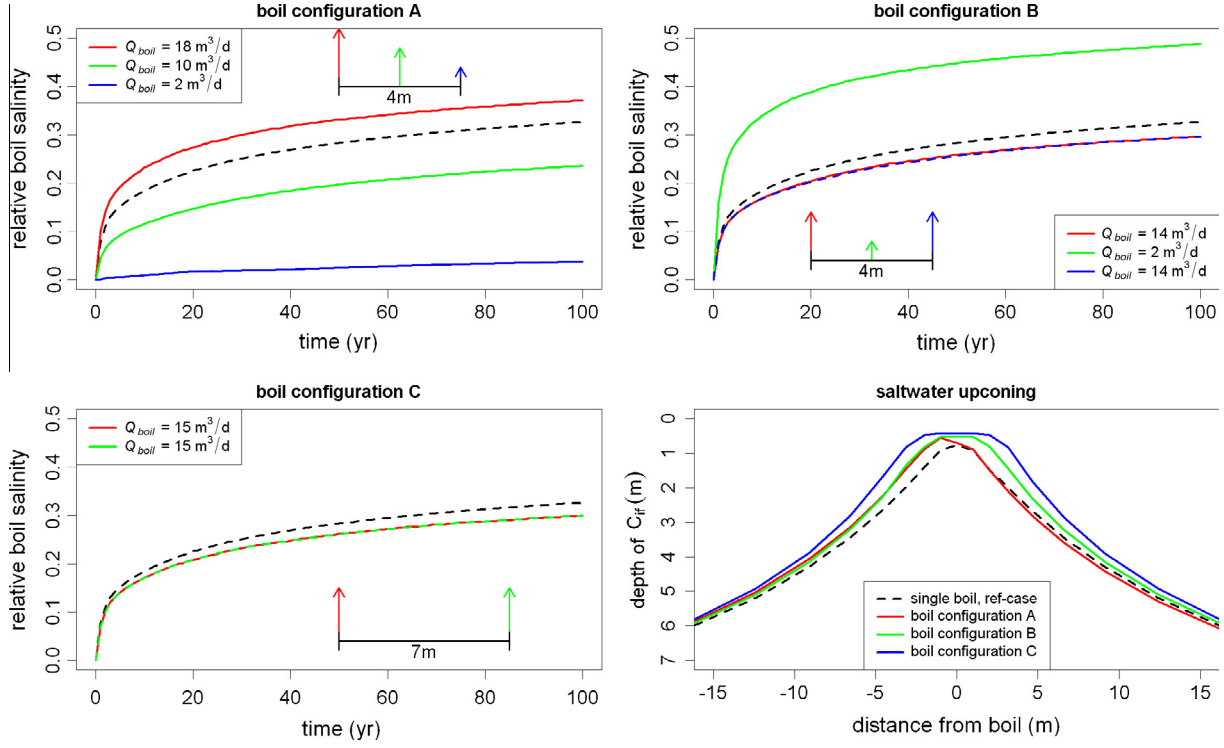

Fig. 9. Boil salinity with time and the saltwater upconing for different boil configurations (A–C). Each boil configuration consists of 2 or 3 boils with different discharges with a total discharge equal to the reference case (Q_{boil} = 30 $m^3\ d^{-1}$). The configuration is indicated with colored arrows. The results of the reference case are indicated by a black dotted line. (For interpretation of the references to color in this figure legend, the reader is referred to the web version of this article.)

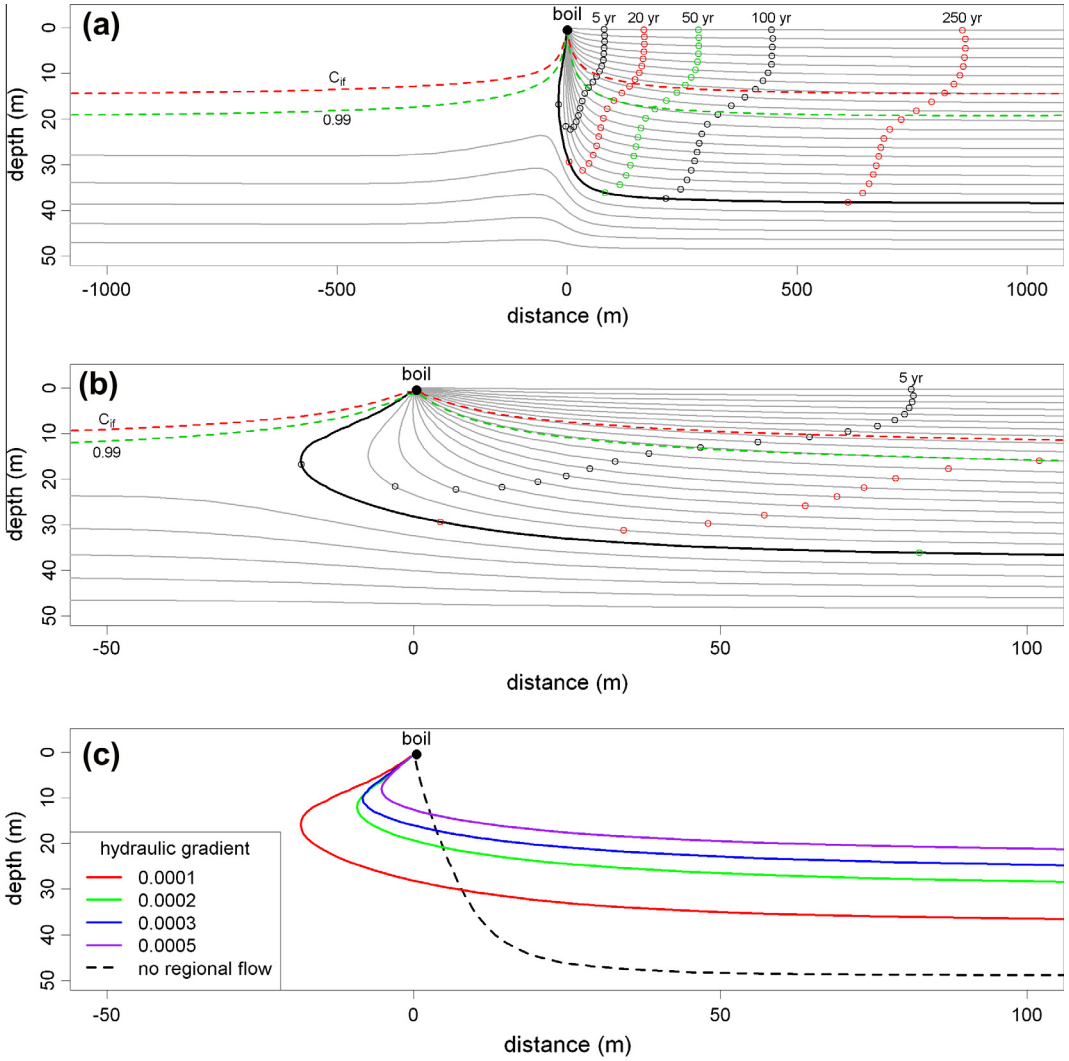

Fig. 10. (a) Streamlines towards the boil with travel times to the boil (in years) for the case with regional flow (hydraulic gradient = 0.0001). The colored points at the streamlines indicate the travel time to the boil. The relative salinity contours of 0.50 (C_{if}) and 0.99 (bottom transition zone) are indicated as well. (b) Same as Fig. 10a but zoomed in. (c) Dividing streamlines for the regional flow cases with different hydraulic gradients and the reference case without regional flow. (For interpretation of the references to color in this figure legend, the reader is referred to the web version of this article.)

aquitard in the manner illustrated in Fig. 1, but rather, it is more likely that they have their own source vents. The development of new boils when boils 1 and 2 were blocked during the sealing experiment implies that new cracks developed in the aquitard or existing cracks within the aquitard were regenerated. The development of new boils indicates that boil sealing is not a feasible measure to abate salinization at these particular sites.

5.2. Sources of boil water

The numerical simulations showed that boil water is a mixture of groundwater from different depths (quantified by CD_i) with different salinities. Mixing is enhanced near the boil where streamlines from different depths and with different salinities converge. To test if CD_i was a valid model output parameter representing the sources (depths) of boil water, the boil salinity after 100 years was calculated with Eq. (1) for all axisymmetric upconing cases listed in Table 1 and compared with the simulated boil salinity. Fig. 11 shows that the boil salinity calculated with Eq. (1) correlates well ($R^2 = 0.96$) with the simulated boil salinity and that CD_i is indeed a good representative for the sources of boil water. The

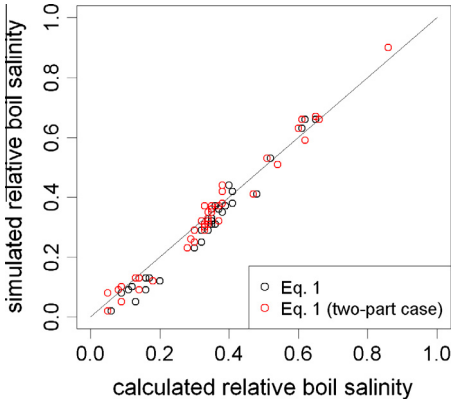

Fig. 11. Scatter diagrams of the calculated boil salinity using Eq. (1) and simplified Eq. (1) (two-part case) versus the simulated boil salinity. The data is derived from the model results of all axisymmetric upconing cases listed in Table 1.

slightly overestimation in calculated values is probably caused by boil salinities not reaching steady state after 100 years (Fig. 5a).

Boil salinity was also calculated with a simplified form of Eq. (1) where $m = 2$, and $i = 1$ and $i = 2$ refer to the part of the aquifer above and below C_{if}, respectively. Fig. 11 shows that the boil salinity calculated using the simplified two-part form of Eq. (1) correlated well with both the boil salinity predicted with the numerical model and the calculated boil salinity using Eq. (1). This confirms that for aquifer salinity distributions with a symmetric transition zone, CD_i is reasonably simplified to one parameter, which is CD_{sh}. Note that in cases without density effects, CD_i is equally distributed within the aquifer and the boil water solute concentration in steady state is simply the average solute concentration in the aquifer. By doing so for the reference case without density effects, a boil salinity of $0.71Cl_s$ is obtained, which is slightly less than the boil salinity of $0.73Cl_s$ predicted by the numerical model.

5.3. Effect of aquifer salinity distribution

There is significant variability in the regional aquifer salinity distributions below Dutch deep polders (Van Rees Vellinga et al., 1981; Oude Essink et al., 2010) showing ranges of C_{if}, W_{if} and β according to the ranges used for the axisymmetric simulations (Table 1). The model results showed that C_{if} and β had a major impact on both CD_{sh} and boil salinity (Fig. 8). Hence, the spatial variations in C_{if} and β in Dutch aquifers are probably important factors causing differences in the salinities of boils in Dutch polders. Variations in K_h and Q_{boil} are also likely to cause differences in boil salinities in Dutch polders, with other parameters (K_v, D, n, α_L, α_T, W_{if}) showing reduced sensitivity (Fig. 8).

In Dutch aquifers with uniform profiles of density, CD_i and the steady-state boil solute concentration are independent of Q_{boil}, K_h, K_v, D and n, which influence more so travel times and the time required to reach steady state. In contrast, by adding density differences, CD_i and therefore boil salinity depend on many factors (Q_{boil}, K_h, K_v, D, n, α_L, α_T, C_{if}, W_{if} and β). The density distribution in an aquifer determines in what magnitude these factors influence upconing. Even with small density differences (e.g. $\beta = 0.0013$, case 12a), density effects cannot be neglected as they still significantly influence CD_{sh} (0.39 for $\beta = 0.0013$; 0.30 for $\beta = 0$) and boil salinity ($0.67Cl_s$ for $\beta = 0.0013$; $0.73Cl_s$ for $\beta = 0$). Fig. 8 shows that β had more impact on boil salinity in the range of small β, which apply for Dutch aquifers below deep polders, than in the range of large β.

Field measurements from this study and by De Louw et al. (2010) and Goudriaan et al. (2011) showed that despite the small discharges, almost all boils discharge water with elevated Cl concentrations of up to 5 g L^{-1}. This observation is consistent with the results of numerical simulations and can be explained by the general shallow position of C_{if} (15–40 m below the aquitard) in combination with relatively small β (Cl_s ranges from 15% to 40% seawater) in the study area. These conditions resulted in significant contributions of saline groundwater below C_{if}.

5.4. Effect of regional flow

The 3D numerical simulations showed that regional lateral flow divides the aquifer into two flow systems; the local boil system on top of the regional flow system. Consequently, boil water comes from shallower depth (i.e. from above the dividing streamline) compared to the situation without regional flow (i.e. from the entire aquifer). Despite this, CD_{sh} and thus boil salinity were barely influenced by the regional flow component. This follows from the fact that regional flow reduces the effective aquifer thickness for the local flow to the boil, bordered by the dividing streamline. And in addition, the axisymmetric results showed that CD_{sh} are barely influenced by aquifer thickness as long as the entire transition zone is completely within the aquifer (Table 4, cases 5a–d). The results imply that boil salinity is not influenced by the position of the boil in the deep polder with respect to the magnitude of regional flow. Regional flow is therefore not an important factor that explains the spatial variability of boil salinities found in the Dutch deep polders.

In most coastal aquifers, regional flow is present to some extent and this is not taken into account in most detailed saltwater upconing models (e.g. Reilly and Goodman, 1987; Ma et al., 1997; Zhou et al., 2005), probably due to large calculation times. Bear et al. (2001) incorporated regional flow in their numerical upconing model but only mentioned the asymmetry of the saltwater cone as an effect of regional flow. Regional flow will significantly affect pumping water salinity when a part of the transition zone or the entire transition zone is found below the dividing streamline. Regarding this positive effect that regional flow could potentially have on saltwater upconing and therefore on pumping well salinities as well, leaving out the regional flow component can be seen as a worse case scenario.

6. Conclusions

In this study, natural saltwater upconing by the preferential groundwater discharge through boils, identified previously as a key process in the salinization of Dutch deep polders, was investigated using field measurements and numerical simulations of simplified situations. For the first time, groundwater salinity distributions attributable to specific boils or boil clusters were measured. The field measurements showed local and steep upconing due to the preferential groundwater discharge of boils. Upconing in numerical models, albeit for idealized situations, showed similar characteristics to field situations.

The numerical results indicated that boil water in Dutch polders comprises mixtures of groundwater from a wide range of depths and salinities. All simulated cases showed a depth-contribution to boil discharge that had a form opposite to the salinity distribution in the aquifer, which illustrates the importance that the salinity (and therefore density) distribution has on saltwater upconing mechanisms. A uniform contribution to boil discharge was produced in simulations with uniform vertical salinity profiles. For aquifers with symmetric transition zones, the contributing depth distribution was well characterized by a two-part model involving only the shallow and deep contribution to boil discharge, defined as the portions of boil water coming from above and from below the center depth of the transition zone, respectively. Regional lateral flow below Dutch polders impacted the flow patterns significantly by dividing the groundwater flow system into a local boil system overlying the regional flow system. Despite this, regional flow had only a minor effect on the shallow and deep contributions and thus on boil salinity as well.

The most important factors controlling the shallow and deep contribution and therefore boil salinities in Dutch deep polders are boil discharge, the horizontal hydraulic conductivity of the aquifer, the depth of the transition zone and the density difference between groundwater above and below the transition zone. The fact that boils in Dutch polders discharge saline groundwater under relatively low discharge conditions can be explained by the shallow position of the transition zone in combination with relatively small density differences within the aquifer. These conditions result in significant contributions of saline groundwater, from below the transition zone, to boil discharge. The observed spatial variation in boil salinities is probably the result of a combination of variations in boil discharge and the spatial variation of aquifer salinity distributions and the horizontal hydraulic conductivity of the aquifer. Additionally, within a small area of clustered boils, boil salinity varies between individual boils and is deter-

mined by the combination of its discharge and its position within the boil area (i.e. relative to neighboring boils), whereas the total discharge of boil clusters is the principal factor that controls natural saltwater upconing and total salt loads. The width of the transition zone, aquifer thickness, porosity, dispersivity and the vertical hydraulic conductivity did not have major effects on the natural saltwater upconing mechanism by boils.

Acknowledgements

We thank Frank van Schaik and Jos van Rooden (Rijnland Water Board), Mike van der Werf (Deltares) and the farmers Avis, Dorrepaal and Steenwijk for their help collecting the field data and Peter Vermeulen (Deltares) and Jackie Leng (Utrecht University) for their contribution to the project. We thank Danica Jakovovic (National Centre for Groundwater Research and Training, Flinders University), Jelle Buma (Deltares) and the anonymous reviewers for their valuable comments on the paper.

References

Archie, G.E., 1942. The electrical resistivity log as an aid in determining some reservoir characteristics. Petrol. Trans. AIME 146, 54–62.

Bear, J., Zhou, Q., Bensaba, J., 2001. Three dimensional simulation of seawater intrusion in heterogeneous aquifers, with application to the coastal aquifer of Israel. In: Proceedings of First International Conference on Saltwater Intrusion and Coastal Aquifers: Monitoring, Modeling, and Management, Essaouira, Morocco, 13pp.

Bower, J.W., Motz, L.H., Durden, D.W., 1999. Analytical solution for determining the critical condition of saltwater upconing in a leaky artesian aquifer. J. Hydrol. 221, 43–53.

Custodio, E., Bruggeman, G.A., 1987. Groundwater Problems in Coastal Areas, Studies and Reports in Hydrology. UNESCO, International Hydrological Programme, Paris.

Dagan, G., Bear, J., 1968. Solving the problem of local interface upconing in a coastal aquifer by the method of small perturbations. J. Hydraul. Res. 6 (1), 15–44.

Diersch, H.J.G., Prochnow, D., Thiele, M., 1984. Finite-element analysis of dispersion-affected saltwater upconing below a pumping well. Appl. Math. Model. 8, 305–312.

De Louw, P.G.B., Oude Essink, G.H.P., Stuyfzand, P.J., Van der Zee, S.E.A.T.M., 2010. Upward groundwater flow in boils as the dominant mechanism of salinization in deep polders, The Netherlands. J. Hydrol. 394, 494–506.

De Louw, P.G.B., Van de Velde, Y., Van der Zee, S.E.A.T.M., 2011a. Quantifying water and salt fluxes in a lowland polder catchment dominated by boil seepage: a probabilistic end-member mixing approach. Hydrol. Earth Syst. Sci. 15, 2101–2117.

De Louw, P.G.B., Eeman, S., Siemon, B., Voortman, B.R., Gunnink, J., Van Baaren, S.E., Oude Essink, G.H.P., 2011b. Shallow rainwater lenses in deltaic areas with saline seepage. Hydrol. Earth Syst. Sci. 15, 3659–3678.

Friedman, P.S., 2005. Soil properties influencing apparent electrical conductivity: a review. Comput. Electron. Agric. 46, 45–70.

Goes, B.J.M., Oude Essink, G.H.P., Vernes, R.W., Sergi, F., 2009. Estimating the depth of fresh and brackish groundwater in a predominantly saline region using geophysical and hydrological methods, Zeeland, the Netherlands. Near Surf. Geophys. 7, 401–412.

Goudriaan, R., De Louw, P.G.B., Kramer, M., 2011. Mapping saline boils in the Haarlemmermeer Polder. H_2O 3, 29–32 (in Dutch).

Holzer, T.L., Clark, M.M., 1993. Sand boils without earthquakes. Geology 21, 873–876.

Jakovovic, D., Werner, A.D., Simmons, C.T., 2011. Numerical modelling of saltwater upconing: comparison with experimental laboratory observations. J. Hydrol. 402, 261–273.

Johannsen, K., Kinzelbach, W., Oswald, S.E., Wittum, G., 2002. The saltpool benchmark problem–numerical simulation of saltwater upconing in a porous medium. Adv. Water Resour. 25, 335–348.

Langevin, C.D., 2008. Modeling axisymmetric flow and transport. Ground Water 46 (4), 579–590.

Langevin, C.D., Thorne, D.T., Dausman, A.M., Sukop, M.C., Guo, W., 2007. SEAWAT Version 4: A Computer Program for Simulation of Multi-species Solute and Heat Transport: U.S. Geological Survey Techniques and Methods. Book 6, 39pp (Chapter A22).

Li, Y., Craven, J., Schweig, E.S., Obermeier, S.F., 1996. Sand boils induced by the 1993 Mississippi River flood: could they one day be misinterpreted as earthquake-induced liquefaction? Geology 24, 171–174.

Ma, T.S., Sophocleous, M., Yu, Y.S., Buddemeier, R.W., 1997. Modeling saltwater upconing in a freshwater aquifer in south-central Kansas. J. Hydrol. 201, 120–137.

Oude Essink, G.H.P., 1996. Impact of Sea Level Rise on Groundwater Flow Regimes. A Sensitivity Analysis for the Netherlands. Ph.D. Thesis, Delft University of Technology, 428pp.

Oude Essink, G.H.P., Van Baaren, E.S., De Louw, P.G.B., 2010. Effects of climate change on coastal groundwater systems: a modeling study in The Netherlands. Water Resour. Res. 46, W00F04. http://dx.doi.org/10.1029/2009WR008719.

Pollock, D.W., 1994. User's Guide for MODPATH/MODPATH-PLOT, Version 3: A Particle Tracking Post-processing Package for MODFLOW, the U.S. Geological Survey Finite-Difference Groundwater Flow Model: U.S. Geological Survey Open-File Report 94-464, 234pp.

Post, V.E.A., 2004. Groundwater Salinization Processes in the Coastal Area of The Netherlands due to Transgressions during the Holocene. Ph.D. Thesis, Free University Amsterdam, 138pp.

Post, V.E.A., Kooi, H., Simmons, C.T., 2007. Using hydraulic head measurements in variable-density ground water flow analyses. Ground Water 45 (6), 664–671.

Post, V.E.A., Abarca, E., 2010. Saltwater and freshwater interactions in coastal aquifers. Hydrogeol. J. 18 (1), 1–4.

REGIS II, 2005. Hydrogeological Model of The Netherlands. Report: Vernes RW, Van Doorn, THM. From Guide Layer to Hydrogeological Unit, Explanation of the Construction of the Data Set. TNO Report NITG 05-038-B, Utrecht, The Netherlands (in Dutch).

Reilly, T.E., Goodman, A.S., 1987. Analysis of saltwater upconing beneath a pumping well. J. Hydrol. 89, 169–204.

TACFD (Technical Advisory Committee on Flood Defenses), 1999. Technical Report on Sand Boils (Piping). Road and Hydraulics Division of the Directorate-General for Public Works and Water Management, The Netherlands.

Van Rees Vellinga, E., Toussaint, C.G., Wit, K.E., 1981. Water quality and hydrology in a coastal region of The Netherlands. J. Hydrol. 50, 105–127.

Van der Eertwegh, G.A.P.H., Nieber, J.L., De Louw, P.G.B., Van Hardeveld, H.A., Bakkum, R., 2006. Impacts of drainage activities for clay soils on hydrology and solute loads to surface water. Irrigat. Drain. 55, 235–245.

Vos, P., Zeiler, F., 2008. Holocene transgressions of southwestern Netherlands, interaction between natural and antrophogenic processes. Grondboor Hamer 3–4 (in Dutch).

Werner, A.D., Jakovovic, D., Barry, D.A., Simmons, C.T., Zhang, H., 2012. Discussion on ''Experimental observations of saltwater up-coning'' by Werner, A.D., Jakovovic, D., Simmons, C.T., 2009. J. Hydrol. 458–459, 118–120.

Werner, A.D., Jakovovic, D., Simmons, C.T., 2009. Experimental observations of saltwater up-coning. J. Hydrol. 373, 230–241.

Zhang, H., Hocking, G.C., Seymour, B., 1997. Critical and supercritical withdrawal from a two-layer fluid through a line sink in a partially bounded aquifer. J. Aust. Math. Soc. Ser. B: Appl. Math. 39, 271–279.

Zhou, Q., Bear, J., Bensabat, J., 2005. Saltwater upconing and decay beneath a well pumping above an interface zone. Transp. Porous Media 61, 337–363.